Combining Coordination of Motion Actuators with Driver Steering Interaction

Kristoffer Tagesson[1,2], Leo Laine[1,2], Bengt Jacobson[1]

[1]Division of Vehicle Engineering & Autonomous Systems,
Chalmers University of Technology
&
[2]Department of Chassis Strategies & Vehicle Analysis,
Volvo Group Trucks Technology
Dept BF72991, AB4S SE-405 08, Göteborg Sweden
kristoffer.tagesson@volvo.com

Abstract

A new method is suggested for coordination of vehicle motion actuators; where driver feedback and capabilities become natural elements in the prioritisation. The method is using a weighted least squares control allocation formulation, where driver characteristics can be added as virtual force constraints. The approach is in particular suitable for heavy commercial vehicles which in general are over actuated. The method is applied, in a specific use case, by running a simulation of a truck applying automatic braking on a split friction surface. Here the required driver steering angle, to maintain the intended direction, is limited by a constant threshold. This constant is automatically accounted for when balancing actuator usage in the method. Simulation results show that the actual required driver steering angle can be expected to match this constant well. Furthermore, the stopping distance is very much affected by the set capability of the driver to handle the lateral disturbance, as expected. In general the capability of the driver to handle disturbances should be estimated in real-time, considering driver mental state. By using the method it will then be possible to estimate e.g. stopping distance implied from this. The set up has the potential of even shortening the stopping distance, when the driver is estimated as active, this compared to currently available systems. The approach is feasible for real-time applications and requires only measurable vehicle quantities for parametrisation. Examples of other suitable applications in scope of the method would be electronic stability control, lateral stability control at launch and optimal cornering arbitration.

Keywords: Driver Interaction; Control Allocation; Actuator Coordination; Split Friction; Heavy Commercial Vehicles; AEBS

INTRODUCTION

Human drivers can effectively adapt and assess new situations. Computer controlled vehicles can do boring things millions of times in a reliable and quick way. A combination of these two is therefore of course appealing when striving for safe vehicles. Systems developed to assist the driver, traditionally known as advanced driver assistance systems, ADAS, are often developed to support the driver in one specific direction longitudinal, lateral, or roll etc. E.g. advanced emergency braking system, AEBS, is controlling the longitudinal motion to avoid collision by braking. Another example is electronic stability control, ESC. Often with the primary objective of

controlling vehicle yaw motion. Since motions are coupled also other directions can be affected. An example is that AEBS, which is soon mandatory on heavy trucks in Europe (European Union, 2012), may cause lateral deviation when activated on a split friction road segment, see (Tagesson et al., 2014). Here, the driver needs to actively steer to reduce this lateral drift induced by uneven brake action. Another example is brake based ESC which causes speed to go down; this might be undesirable when travelling uphill. When affecting motions in other directions than the primary one it is important to balance the assistance to guarantee at least safety. In this paper we look at how to handle and limit such disturbances induced via coupled motions, using a generic approach. We only consider vehicles with a mechanical connection between driver steering interface and front wheels. The methods developed are in particular suitable for heavy commercial vehicles or heavy vehicle combinations. In general, these have more actuators than controlled motions. This implies that actuator coordination is needed. Previous research has suggested control allocation, CA, methods as a structured way of including a variety of motion actuators to coordinate for the desired motion of the vehicle or even articulated vehicle combination, see e.g. (Tagesson et al., 2009; Uhlén et al., 2014; Tjønnås and Johansen, 2010). CA makes it possible to achieve a modularized control architecture, where high level control modules determine the control objective of the motion and lower level modules allocate forces amongst actuators. The methods are feasible in real time, see (Tagesson et al., 2009), and can be extended to a model predictive control formulation in order to include actuator dynamics, see (Luo et al., 2007).

Manning and Crolla (2007) summarises state of the art methods for lateral control of passenger vehicles. More or less all methods work according to the following principle, determine what the intention of the driver is then control the vehicle such that this is achieved, while maintaining stability. The same principle can be observed also for CA applications, like in (Doumiati, 2011; Knobel, 2009; Tjønnås and Johansen, 2010). For modern vehicles equipped with ADAS systems the situation is somewhat different. It is not only the intention of the driver that is triggering controls. E.g. AEBS can trigger heavy deceleration in order to avoid collision. If this action causes disturbances via coupled motions, we can consequently not rely on the driver only, unless we limit theses disturbances to a safe level. A connection between the driver and the CA layer is missing. The objective here is to develop a method for this; where motion actuators are coordinated to maximize the manoeuvrability and stability of the truck and where driver feedback and capabilities become natural elements. This is the focus of this paper.

The paper is structured as follows. First the generic principle of the method is described. This is followed by simulations of the scenario AEBS activated on a split friction road to exemplify the usage of the method. A final discussion concludes the findings and the results. Sign conventions used are compliant with ISO 8855, ISO (1991). Units are SI unless otherwise stated.

METHODS

An important starting point for CA is that the equations of motions for the vehicle can be approximated with an affine state space form

$$\dot{x} = g(x) + h(x)u \tag{1}$$

with a k-dimensional state vector x, furthermore g and h as general functions, and the m-dimensional actuator vector u, composed from e.g. brake torques, engine torque and rear-axle steering angle. If a sufficiently short time interval is considered it further holds that $h(x)u \approx Bu$, with $B \in \Re^{k\times m}$ known as the *control effectiveness matrix*. The basics in CA is to achieve

$$\{Bu = v \mid u_{min} \leq u \leq u_{max}\} \tag{2}$$

where v is the *virtual control vector*. For road vehicle planar motion control v is preferably composed from resulting longitudinal force F_x, resulting lateral force F_y, yaw torque M_z, and possible trailer counterparts, (Uhlén et al., 2014).

After having made the substitution from actuator dependent properties to a virtual control vector the problem is decoupled. Firstly, a motion control part considering the system $\dot{x} = g(x) + v$. Secondly, a control allocation part trying to achieve $Bu = v$ and thus making the residual $Bu - v = 0$. Since u is constrained the latter is not always possible. The residual then becomes a measure of the infeasibility in virtual control request. Since v normally is a selection of resulting forces and torques that counteracts it is sometimes possible to constrain the residual according to

$$v_{min} - v \leq Bu - v \leq v_{max} - v \tag{3}$$

where v_{min} and v_{max} are vectors of size k. These can both be used in the motion control part to limit disturbances

via coupled motions, as will be explained more in detail below.

The decoupling achieved is visualised graphically in Fig. 1 where the main architecture of the developed method is shown, including v_{min} and v_{max} limitations and residual propagation. In this figure yet another decoupling is introduced, namely actuator control. For each actuator i there is a block with the input u_i and an estimation of the limitations $u_{min,i}$ and $u_{max,i}$. The different parts of Fig. 1 will now be explained more in detail starting from the bottom and up. As mentioned previously an implementation of AEBS will be used to exemplify the usage of the method. It is set up for a 6×2 rigid truck having one brake actuator per wheel. Fig. 2 show a more detailed version of the main architecture as used in this AEBS example. The details will be explained along with the example.

Actuator Control

For each actuator included in the controls there is a function handling local control of the actuator. Both range estimation and error-controlled regulation should be included.

As seen in Fig. 2 six brake actuators are used in the AEBS implementation. A longitudinal force request, $F_{xri} = u_i$, is input to the actuator belonging to wheel i. In the remainder the index $i = \{1,2,3,4,5,6\}$ is denoting, in order, front left, front right, drive (first rear axle) left, drive right, tag (second rear axle) left or tag right. This request is simply multiplied by the effective wheel radius R_e to form the resulting wheel torque. The effective wheel radius can be estimated from a free rolling wheel as $R_e = v_x/\omega_{wi}$, where v_x is vehicle longitudinal speed, ω_{wi} wheel speed. To avoid excessive wheel slip a scale factor f_i is used according to

$$f_i = 1 - 100 \cdot \left(\left| \frac{v_x - R_e \cdot \omega_{wi}}{v_x} \right| - 0.1 \right) \tag{4}$$

$$T_i = \begin{cases} R_e F_{xri}, & \text{if } f_i \geq 1 \\ f_i R_e F_{xri}, & \text{if } 0 < f_i < 1 \\ 0, & \text{if } f_i \leq 0 \end{cases} \tag{5}$$

where v_{xi} is wheel longitudinal speed and T_i wheel torque which is applied directly to the wheel. The value 0.1 reflect peak friction slip level.

Friction is assumed known when estimating the brake force ranges according to

$$u_{min,i} = -\mu_i F_{z,i} \tag{6}$$

where μ_i is the current friction level at wheel i and $F_{z,i}$ is the current vertical force at wheel i. The maximum brake force $u_{max,i}$ is set to 0. This makes the actuator capability vector $F_{xci} = [-\mu_i F_{z,i}, 0]$.

Control Allocation Formulation

As mentioned there is in general no guarantee for an existing u to fulfil Eq. (2). When no solution exists some arbitration rule has to be applied. In CA a common way is to minimize the weighted norm $\|W_v(Bu - v)\|_2$. Here specifically the ℓ_2-norm, for alternatives see (Laine, 2007). On the other hand if the solution is not unique as $dim(v) < dim(u)$ some secondary rule has to be introduced, to achieve uniqueness. By using a weighted ℓ_2-norm also for this the weighted least squares problem for CA can be formulated as

$$\begin{aligned} u = &\arg\min(\|W_u(u - u_d)\|_2^2 + \gamma\|W_v(Bu - v)\|_2^2) \\ &\text{subject to } u_{min} \leq u \leq u_{max} \end{aligned} \tag{7}$$

where W_u and W_v are weighting matrices, u_d is a desired set point of the actuator vector u, and γ is a high scalar weight to emphasise the importance of achieving a small residual. More details about this formulation can e.g. be found in (Härkegård, 2003).

In particular the W_v matrix can be used to emphasis what force or torque in v that is of highest importance to fulfil. All other terms will be subordinate. This can make this traditional formulation of CA, as in Eq. (7), hard to use in practise. A particular element in v can often be prioritised, however all other elements cannot be

fully subordinate, i.e. released. Getting back to the AEBS implementation running on split friction it is clear that deceleration is prioritised, but the induced yaw torque must be limited. As previously suggested in Eq. (3) this can be achieved by adding extra constraints according to

$$\begin{aligned} u = &\arg\min(\|W_u(u-u_d)\|_2^2 + \gamma\|W_v(Bu-v)\|_2^2) \\ &\text{subject to } u_{min} \leq u \leq u_{max} \quad \& \quad v_{min} \leq Bu \leq v_{max} \end{aligned} \tag{8}$$

With this formulation it is possible to prioritise a specific element in v, using W_v, at the same time as limitations are put on other elements, using v_{min} and v_{max}. The choice of v_{min} and v_{max} must however be made with some caution in order to make sure that the feasible set is non-empty. In the AEBS example this is guaranteed since $u_{min} \leq \mathbf{0} \leq u_{max}$ and $v_{min} \leq \mathbf{0} \leq v_{max}$. Thus a trivial solution exists and guarantees a non-empty feasible region. In a more general case there is no explicit way of showing this property, there are however iterative methods for this, e.g. Simplex Phase I, (Nocedal and Wright, 2006).

An Active Set solver, implemented in Matlab m-code, was developed for solving Eq. (8). The solver will be uploaded to Matlab Central File Exchange for public access. It is marked with hashtag #tagessonwlssolver. The solver was run on a dSpace Micro Autobox II to test real-time feasibility. The worst case turnaround time observed for producing a solution was 0.15 ms. C.f. 0.06 ms which was achieved in a similar set-up when using a C version Active Set solver for solving Eq. (3) in (Tagesson et al., 2009). Common for vehicle motion control systems like ESC and AEBS is to run at ~ 10 ms.

In the AEBS implementation the virtual control vector used is

$$v = \begin{bmatrix} F_{x,req} \\ M_{z,req} \end{bmatrix} \tag{9}$$

where $F_{x,req}$ is the desired resulting longitudinal force and $M_{z,req}$ is the desired resulting yaw torque. We assume small slip angles of wheels and no combined slip relation in the allocation. This makes the control effectiveness matrix become

$$B = \begin{bmatrix} 1 & 1 & 1 & 1 & 1 & 1 \\ \frac{-w_f}{2} & \frac{w_f}{2} & \frac{-w_d}{2} & \frac{w_d}{2} & \frac{-w_t}{2} & \frac{w_t}{2} \end{bmatrix} \tag{10}$$

The weighting matrices used are

$$W_v = diag\begin{bmatrix} 1000 & 1 \end{bmatrix} \tag{11}$$

$$W_u = \sqrt{mg}\, diag\left[\frac{1}{\sqrt{F_{z,f}}} \; \frac{1}{\sqrt{F_{z,f}}} \; \frac{1}{\sqrt{F_{z,d}}} \; \frac{1}{\sqrt{F_{z,d}}} \; \frac{1}{\sqrt{F_{z,t}}} \; \frac{1}{\sqrt{F_{z,t}}}\right] \tag{12}$$

as suggested in (Tagesson et al., 2009). The units of W_v is $diag[1/N, 1/Nm]$ and for W_u all elements have the unit $1/N$. All other CA parameters used in the implementation can be found in Table 1 and Table 2.

Motion Control

There are many tasks that a motion controller can be used for. As seen in (Manning and Crolla, 2007) it is a subject on its own. The important aspect to be stressed here is depicted in Fig. 1. The motion controller should not only control the primal motion of interest but should also limit other degrees of freedom that can be affected. This can be done using v_{max} and v_{min}.

In Fig. 1 one arrow indicates the residual $Bu - v$ as propagated to the Motion Control layer. This information can be used for supporting the driver in negotiating induced coupled forces. For instance by adding a supporting torque T_{as} onto the steering wheel. This is however not used in the simulations that follow.

In the AEBS implementation the motion control layer, see Fig. 2, receives a request of longitudinal acceleration $a_{x,req}$ from AEBS logics located on the ADAS layer. This request is simply multiplied with the vehicle mass m to form $F_{x,req}$, i.e. an open-loop acceleration controller. When braking it is not desirable to induce yaw torque, hence $M_{z,req} = 0$ is used. If however yaw torque is induced anyway this should be limited according to what the driver can handle. Assuming that the driver is able to produce a steering wheel angle, δ_d, equal to a set value δ_{as}, where the index *as* denote *anti-steer*, it is possible to estimate how much yaw torque that the driver can reach. A simple way is to use a steady state planar linear vehicle model. It can easily be shown that an applied yaw torque

is cancelled out from steering when

$$M_z = \underbrace{\frac{c_f l_f}{i_s}\left(1+\frac{c_r l_r - c_f l_f}{l_f(c_f+c_r)}\right)}_{=K_{as}}\delta_d \tag{13}$$

where c_f and c_r is effective front respectively rear cornering stiffness, l_f and l_r is the distance from vehicle centre of gravity to front respectively rear axle, and i_s is steering gear ratio. As seen it is possible to group parameters and define a constant parameter K_{as} which can be tuned for a specific vehicle. Using this model and assuming that the driver can steer at most $\pm\delta_{as}$ we get

$$v_{max} = -v_{min} = [\infty\ ,\ K_{as}\delta_{as}]^\intercal \tag{14}$$

RESULTS

A series of simulations were performed including a high-fidelity truck model, developed by Volvo, and the implementation of the AEBS structure as presented. The simulations were run under split-friction conditions on a straight road.

Simulation Set-up

The high-fidelity truck model is shown in Fig. 3. It includes e.g. magic tyre formula tyre model with relaxation, frame twist, suspension, rotating wheels and has been validated extensively. The main parameters of the model are shown in Table 1. Peak friction, μ, was set to 1.0 under left side wheels and 0.2 under the right side wheels. The model and all other parts in the simulations run in Matlab Simulink.

A PID controller was used to control the steering wheel angle. The target of the controller was to keep the vehicle centre of gravity lateral position, Y, as low as possible, this was also the only input to the controller. Having this set-up it is possible to determine how much steering that is required to fully remove a yawing torque. Used proportional gain was 1.1 rad/m, integral gain was 0.44 rad/(m·s) and derivative gain was 0.22 rad·s/m.

AEBS braking was activated after one second, where $a_{x,req}$ was ramped up to -6 m/s^2 after first passing a first order low-pass filter taking account for actuator dynamic, with time constant 0.1 s. Allowed yaw torque was varied by altering anti-steer level according to $\delta_{as} = \{10, 20, 40, 60\}$ deg. The initial speed was set to 22.2 m/s (80 km/h). To avoid numerical problems $a_{x,req}$ was ramped down to zero, using the same filter as for ramp-up, when speed dropped below 4 m/s (14.4 km/h).

Simulation Results

Fig. 4 and Fig. 5 show how the implementation performs in simulation. First of all the longitudinal speed is shown in Fig. 4a. As seen the speed drop is heavily influenced as the allowed yaw torque is altered. Looking at the longitudinal acceleration shown in Fig. 4b the same trends can be seen. The request $a_{x,req} = -6$ m/s^2 is never reached. The $\delta_{as} = 60$ deg line is close to -5 m/s^2, which is almost as low as what is possible to ever achieve considering friction level and load transfer.

In Fig. 4c the steering profile performed by the PID controller is shown. It can be seen that δ_d is close to the programmed value of δ_{as} in steady state. There are some oscillations, but the overall profile is close to δ_{as}. Fig. 4d show the lateral deviation. As seen it is held at a low level, meaning that the PID steering controller works as intended. Fig. 5a and Fig. 5b together show the residual resulting from CA, i.e. the difference between the requested and allocated longitudinal force and yaw torque respectively. As seen M_z is limited by v_{max} almost constantly. Whereas $F_x - F_{x,req}$ is lowered as more yaw torque is allowed.

To underline the severity of the scenario yet another simulation was run where no steering was performed. The lateral position can be seen in Fig. 6. The two cases $\delta_{as} = 40$ deg and $\delta_{as} = 60$ deg both end up at 90 deg sideslip and a lateral deviation of more than 20 m. In the other two cases, $\delta_{as} = 10$ deg and $\delta_{as} = 20$ deg, the lateral deviation is reduced and both end up heading forwards.

DISCUSSION

As clearly shown by simulation it is possible to induce severe disturbances in secondary vehicle states when conditions are imperfect. As the driver is supposed to handle these disturbances it is out-most important to estimate the ability of him/her to do so and thereafter balance the coordination amongst actuators. We present an extended control allocation method where motion actuators are coordinated in accordance to what is: requested, available, and where driver feedback and capabilities become natural elements. The capability of the driver to handle a yaw disturbance, in the AEBS use case, was expressed in terms of the required maximum driver steering wheel angle. The simulation results show that this limit actually roughly was achieved. In other vehicle control approaches, as seen in e.g. Manning and Crolla (2007), this natural way of taking account for driver capabilities is not seen. For brake systems in heavy vehicles as of today the difficulties on split friction is handled by an axle brake limiting approach which cannot account for dynamic driver characteristics. This new set up has the potential of shortening the stopping distance, when the driver is estimated as active. Also when using the suggested method, it is beneficial to constantly estimate the capability of the driver to handle disturbances. In the AEBS case for instance this will have a direct connection to the stopping distance which preferably should be accounted for also in the higher level decision making layer triggering AEBS activation.

Another benefit of the method is that it is independent on vehicle configuration. Meaning that it is possible to derive settings from physical properties and dimensions. The method was also shown suitable for real-time usage.

For future work we suggest a more realistic assumption about the knowledge of friction. We also stress the possibility of guiding the driver using steering wheel torque by means of the residual calculated in the allocation step. Furthermore when involving more actuators, like steering and power-train, the actuator dynamics will prove more important to account for. Other possible applications of the method, apart from AEBS, would be electronic stability control, lateral stability control at launch and optimal cornering arbitration.

References

Doumiati M, Sename O, Martinez JJ, et al. Vehicle yaw control via coordinated use of steering / braking systems. In: 18th IFAC World Congress (IFAC WC 2011). IFAC; 2011:644–649.

European Union. Commission regulation (EU) No 347/2012 of April 2012. 2012.

Härkegård O. Backstepping and control allocation with application to flight control. 2003;(820).

ISO. International standard 8855, Road vehicles and road holding ability - Vocabulary. 1991;1991.

Knobel C. Optimal control allocation for road vehicle dynamics using wheel steer angles, brake/drive torques, wheel loads and camber angles. 2009.

Laine L. Reconfigurable motion control systems for over-actuated road vehicles. 2007.

Luo Y, Serrani A, Yurkovich S. Model-predictive dynamic control allocation scheme for reentry vehicles. J Guid Control Dyn. 2007;30(1):100–113.

Manning W, Crolla D. A review of yaw rate and sideslip controllers for passenger vehicles. Trans Inst Meas Control. 2007;29(2):117–135.

Nocedal J, Wright SJ. Numerical Optimization. 2nd ed. New York: Springer; 2006.

Tagesson K, Jacobson B, Laine L. Driver response to automatic braking under split friction conditions. In: 12th International Symposium on Advanced Vehicle Control. Tokyo, Japan: JSAE; 2014:666–671.

Tagesson K, Sundström P, Laine L, Dela N. Real-time performance of control allocation for actuator coordination in heavy vehicles. In: Intelligent Vehicles Symposium. Xian, China: IEEE; 2009:685–690.

Tjønnås J, Johansen TA. Stabilization of automotive vehicles using active steering and adaptive brake control allocation. IEEE Trans Control Syst Technol. 2010;3(18):545–558.

Uhlén K, Nyman P, Eklöv J, Laine L, Sadeghi Kati M, Fredriksson J. Coordination of actuators for an A-double heavy vehicle combination. In: 17th International IEEE Conference on Intelligent Transportation Systems. IEEE; 2014.

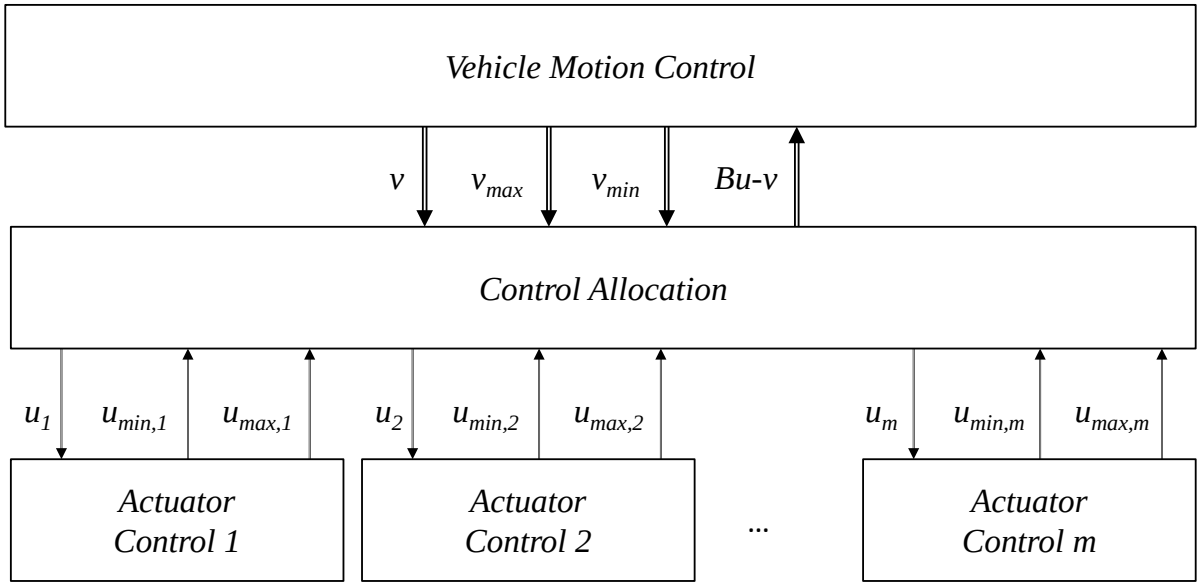

Figure 1: The used control architecture has a decoupled control strategy where actuators are grouped into resulting vehicle forces and torques, v, above the control allocation layer. The vector u is generally composed from a mix of quantities, typically shaft torques on wheels, brake torque on wheels and steering angles of axles. Double line arrows indicate vector signals and single line arrows scalar signals.

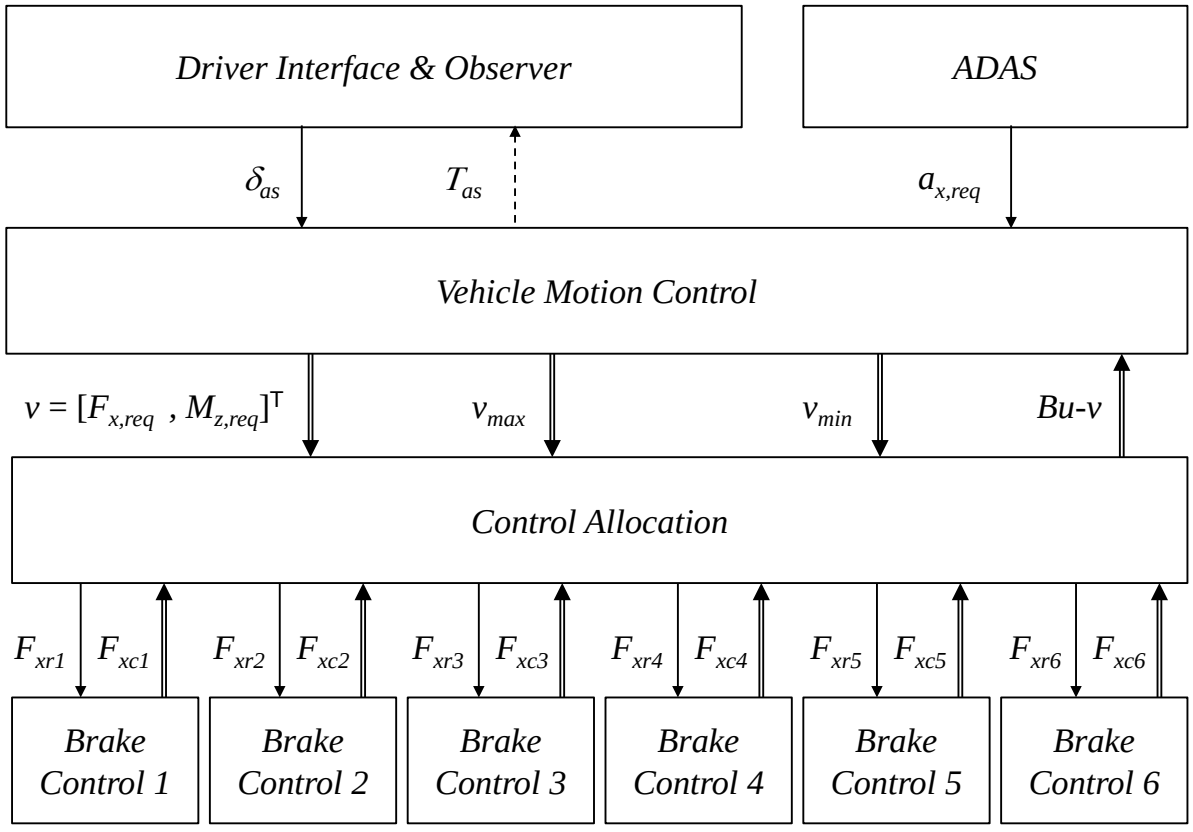

Figure 2: Control architecture as used in AEBS example.

Table 1: Specification of 6×2 truck vehicle model. The axles are refereed to as in order front, drive and tag, meaning first, second and third.

Property	Value	Unit	Description
m	25460	kg	Vehicle mass
L	4.8	m	Wheelbase, distance between front and drive axle
b_s	1.37	m	Boogie spread, distance between drive axle and tag axle
h_{cog}	1.66	m	Sprung body centre of gravity height
$F_{z,f}$	71220	N	Front axle vertical load at standstill
$F_{z,d}$	118111	N	Drive axle vertical load at standstill
$F_{z,t}$	60430	N	Tag axle vertical load at standstill
i_s	23	-	Steering ratio, road wheel angle to StW angle
R	0.5	m	Wheel radius
w_f	2.05	m	Front axle track width
w_d	1.85	m	Drive axle track width
w_t	2.05	m	Tag axle track width

Table 2: Controller specific parameters used in the AEBS implementation.

Property	Value	Unit	Description
g	9.81	kg	Vehicle mass
γ	100	-	CA weight
u_d	$[0,0,0,0,0,0]^\intercal$	N	Actuator set-point
K_{as}	8.47×10^4	Nm/rad	Anti-steer gain
R_e	0.525	m	Effective wheel radius

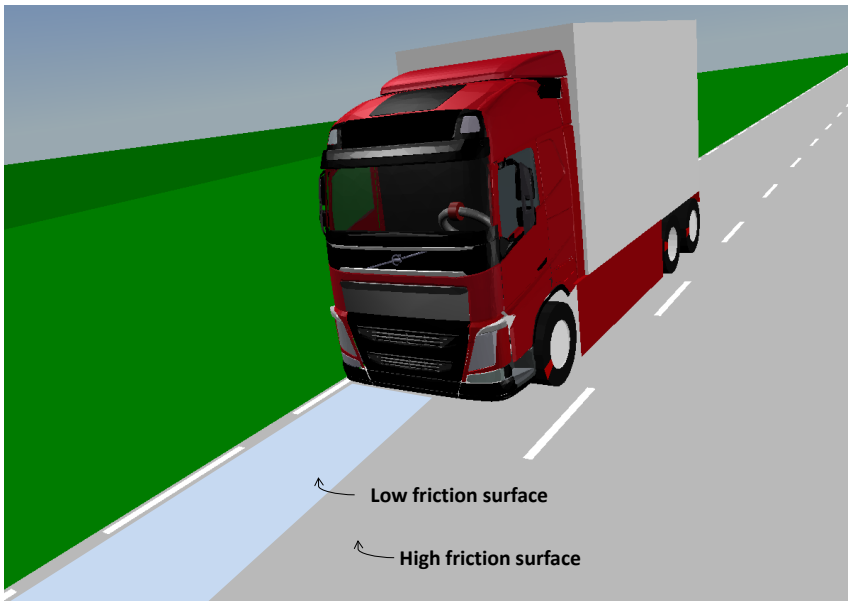

Figure 3: A 6×2 truck model was used in the simulations for the AEBS implementation running on split friction.

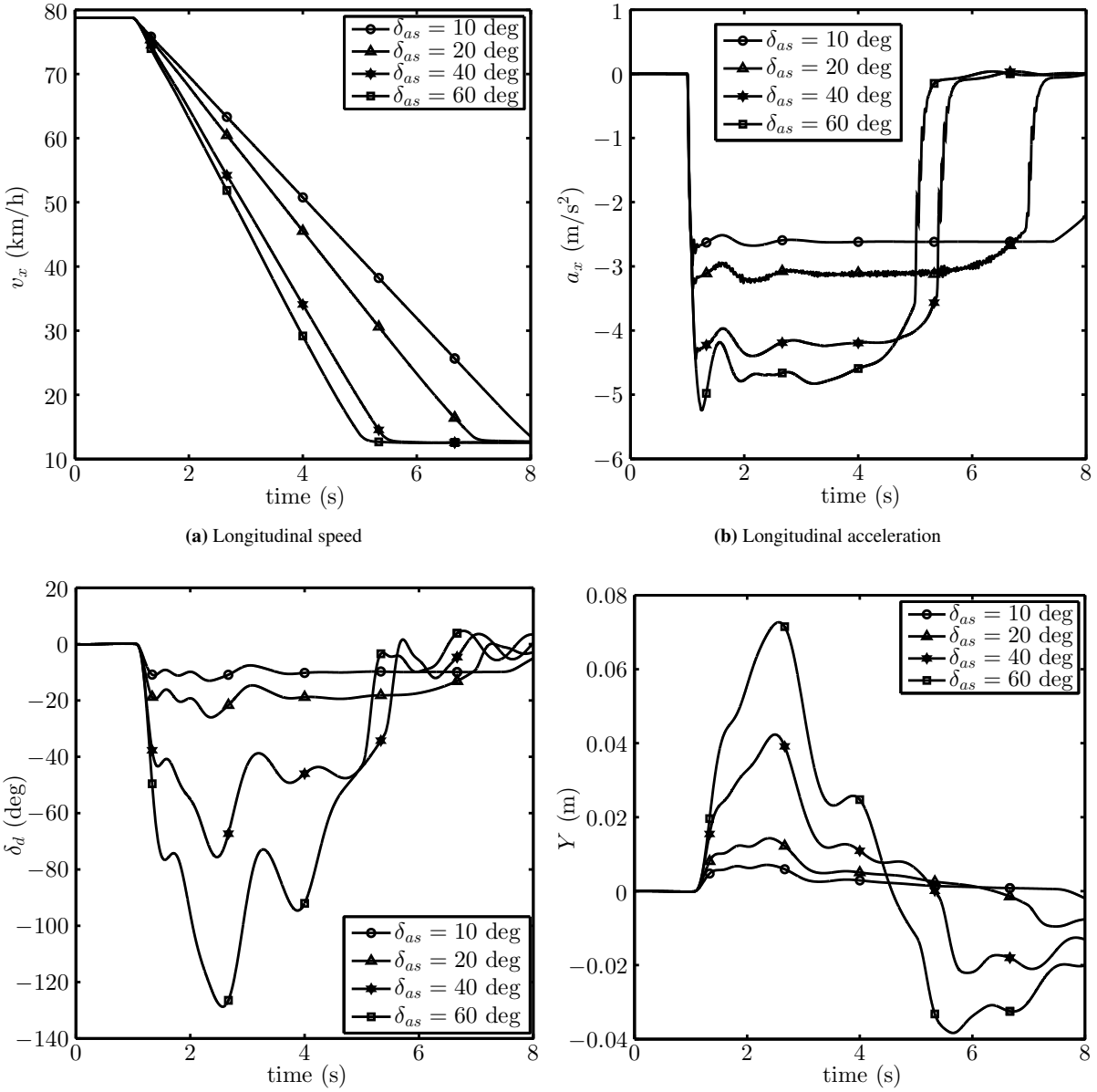

(a) Longitudinal speed

(b) Longitudinal acceleration

(c) Steering wheel angle

(d) Lateral position

Figure 4: Simulation of the AEBS example run on split friction. The required steering action by the driver agree roughly with what has been configured.

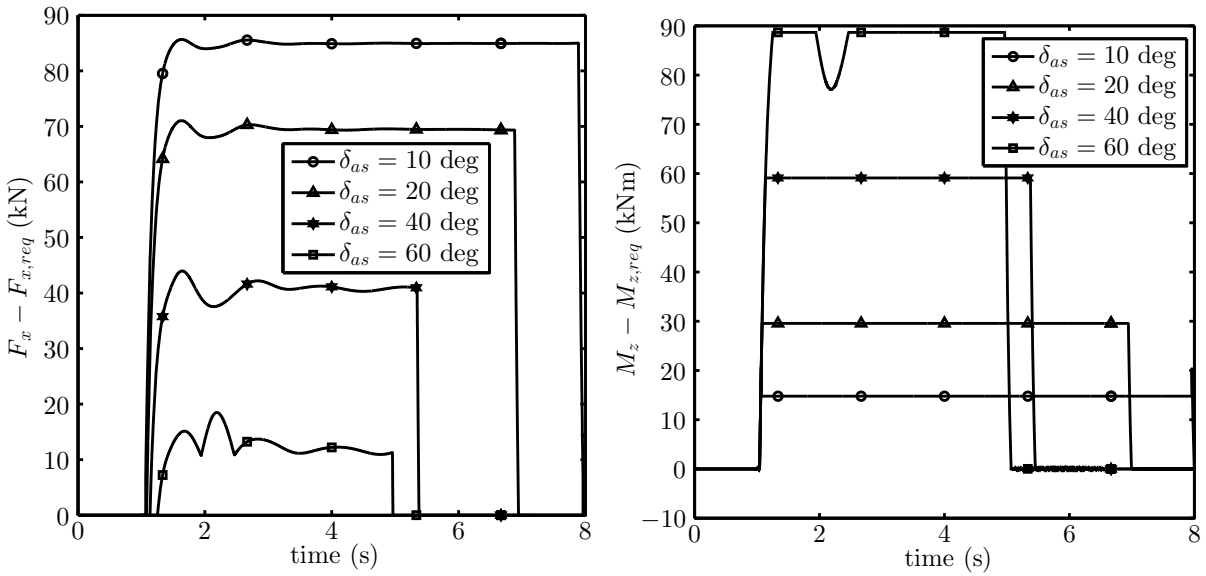

(a) Longitudinal force residual

(b) Yaw torque residual

Figure 5: The residual achieved when running AEBS on split friction. As seen the error in longitudinal force is highly linked to the set limit of yaw torque.

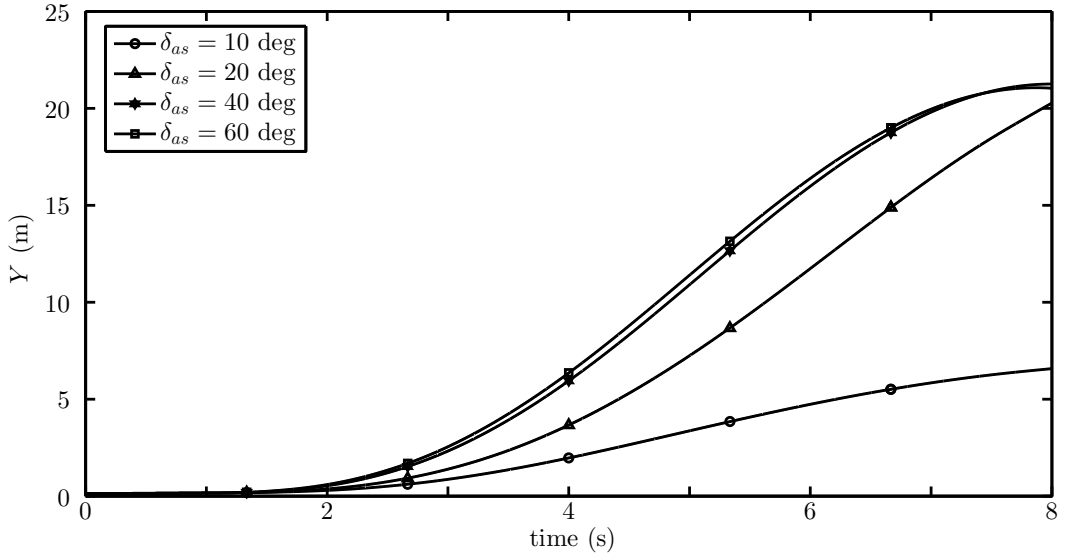

Figure 6: Lateral position shown when no steering action is performed.